PHYSICAL REVIEW B VOLUME 48, NUMBER 8 15 AUGUST 1993-II

Photonic band structures of optically anisotropic periodic arrays

I. H. H. Zabel*
Department of Physics and Byrd Polar Research Center, The Ohio State University, Columbus, Ohio 43210

D. Stroud
Department of Physics, The Ohio State University, Columbus, Ohio 43210
(Received 14 September 1992; revised manuscript received 24 February 1993)

We use a plane-wave expansion to calculate the photonic band structures of anisotropic dielectric composites. The composites consist of a periodic array of anisotropic dielectric spheres embedded in air. Calculations are carried out for spheres that are optically uniaxial or biaxial, Faraday active, or naturally optically active. Anisotropy in the sphere dielectric function is found to split degenerate bands and to narrow or even close band gaps, analogous to Stark or Zeeman splitting in conventional band structures. At long wavelengths, the lowest bands are well described by effective indices of refraction, which are in fairly good agreement with an anisotropic Maxwell-Garnett approximation.

I. INTRODUCTION

It has recently been discovered[1-10] that periodic binary composites can exhibit photonic band gaps, that is, frequency regimes in which an electromagnetic wave cannot propagate, even though the individual constituents allow propagation at these frequencies. These gaps are thus the result of interference effects in a periodic lattice. The dispersion curves for electromagnetic waves can be obtained by band-structure calculations. These reveal that band gaps are most likely when the incident wavelength, the scatterer size, and the composite lattice constant are comparable.[5,11] A typical geometry involves macroscopic grains with dielectric constant ϵ_1, periodically distributed, and embedded in a material with a different dielectric constant, ϵ_2. These scatterers can be considered as photonic "atoms," and the composite as a photonic "crystal."

Scattering from periodic arrays of dielectric objects has been studied for many years.[12] Numerous groups[13] have calculated long-wavelength optical properties of periodic arrays. The concept of a photonic band structure is a relatively recent and convenient idea. Such band structures are relevant at wavelengths comparable to the scatterer size, a regime which is otherwise difficult to treat. The possibility of photonic band gaps opens up the possibility of new devices, such as extremely efficient semiconductor lasers[1,7,8,14] and filters that span previously inaccessible frequency ranges.[1,15]

In this paper we report calculations of photonic band structures for composites with *anisotropic* dielectric constants. Our starting point is a diamond lattice of close-packed dielectric spheres embedded in air. In the isotropic case, it is believed that this lattice exhibits a finite gap.[5,16] Our goal is to investigate how the gap changes when the spheres have anisotropic dielectric constants. We consider uniaxial, biaxial, Faraday active, and naturally optically active spheres. In each case, the dielectric constant of the sphere is no longer a scalar but a second rank tensor $\overleftrightarrow{\epsilon}_s$. (For uniaxial and biaxial materials, $\overleftrightarrow{\epsilon}_s$ is diagonal with unequal diagonal elements. Optically active and Faraday-active materials have a nondiagonal but Hermitian $\overleftrightarrow{\epsilon}_s$. In all cases we assume frequency-independent elements ϵ_{ij} and no absorption, i.e., Hermitian[17] $\overleftrightarrow{\epsilon}_s$ with positive diagonal elements.)

We find that anisotropy in $\overleftrightarrow{\epsilon}_s$ generally tends to reduce the band gap of photonic crystals by breaking the degeneracies of bands with different polarizations. Sufficient anisotropy can close the gap altogether. By varying the anisotropy one can tune the width of the gap along various directions in k space. Using this gap tunability, one may thus be able to build structures which differentially filter out waves of different polarizations.

This paper is divided into sections as follows. Section II describes the anisotropies and model composites to be considered. In Sec. III we discuss the details of our band-structure calculations. We present the results for uniaxial and biaxial spheres in Sec. IV, and for Faraday-active and naturally optically active materials in Sec. V. Finally, we discuss our conclusions in Sec. VI.

II. MODEL

A material may exhibit optical anisotropy either because its structure is anisotropic or because an appropriate symmetry-breaking field is applied.[17] Materials with anisotropic structures may be uniaxial or biaxial, depending on whether their dielectric tensors have two or three distinct principal values. An isotropic material may also become uniaxial under application of a dc electric field (Kerr or Pockels effect). Faraday-active materials can be structurally isotropic, but in the presence of an external magnetic field they rotate the plane of polarization of linearly polarized light. Naturally optically active materials behave similarly, but in the absence of an applied field. Such materials can be structurally isotropic but lack inversion symmetry, because, for example, they contain unequal numbers of left- and right-handed molecules.

The most general relation between $\mathbf{D}$ and $\mathbf{E}$ in a linear

0163-1829/93/48(8)/5004(9)/$06.00

medium is

$$D_i=\sum_{j=1}^{3}\epsilon_{ij}E_j\ , \tag{1}$$

where ϵ_{ij} is a component of the dielectric tensor ϵ. In an isotropic medium, ϵ_{ij} is a multiple of the unit tensor, $\epsilon_{ij}=\epsilon\delta_{ij}$. In a uniaxial or biaxial material, ϵ_{ij} is typically a symmetric matrix with two or three distinct eigenvalues. In an isotropic Faraday-active material, $\mathbf{D}$ and $\mathbf{E}$ are related by

$$\mathbf{D}=\epsilon\mathbf{E}+i\beta\mathbf{E}\times\hat{\mathbf{H}}\ , \tag{2}$$

where $\hat{\mathbf{H}}$ is a unit vector in the direction of the applied magnetic field $\mathbf{H}$, and $\beta\propto H$. A material with natural optical activity (such as quartz, dextrose, cocaine, and strychnine)[18] has a dielectric function which is a real-space operator of the form (for isotropic materials)

$$\epsilon_{ij}(\mathbf{r})=\epsilon^{(0)}\delta_{ij}+\eta\epsilon_{ijl}\frac{\partial}{\partial r_l}\ . \tag{3}$$

Here all indices refer to Cartesian components from 1 to 3, e_{ijl} is the totally antisymmetric unit tensor of rank 3 (Levi-Cività symbol), and a sum over repeated indices is implied. Equation (3) is valid in the limit $\eta k\ll 1$, where k is the wave vector of a propagating electromagnetic wave.

An ordered composite can exhibit a photonic band gap only if the dielectric contrast is large (>4, according to Ho, Chan, and Soukoulis[5]). In what follows, we will describe model calculations for anisotropic composites in which this condition is satisfied. Although the calculations are not directed at specific materials, these conditions can be satisfied in practice, as will be discussed further below.

III. FORMALISM

We consider a periodic composite whose constituents have dielectric tensors $\tilde{\epsilon}_m$ and $\tilde{\epsilon}_s$, and seek solutions to Maxwell's equations which have the form imposed by Bloch's theorem.[19] The relevant Maxwell equations take the form (in the absence of free current density)

$$\nabla\times\mathbf{H}=\frac{1}{c}\frac{\partial}{\partial t}(\tilde{\epsilon}\mathbf{E})\ , \tag{4}$$

where the position-dependent dielectric tensor $\tilde{\epsilon}\equiv\tilde{\epsilon}(\mathbf{r})=\tilde{\epsilon}_m$ or $\tilde{\epsilon}_s$ depending on whether point $\mathbf{r}$ is in medium m or s, and

$$\nabla\times\mathbf{E}=-\frac{1}{c}\frac{\partial\mathbf{B}}{\partial t}\ . \tag{5}$$

Combining these, taking the magnetic permeability $\mu=1$, and assuming that all fields have an $e^{-i\omega t}$ time dependence yields

$$\nabla\times[\tilde{\epsilon}^{-1}(\mathbf{r})(\nabla\times\mathbf{H})]=\frac{\omega^2}{c^2}\mathbf{H}\ , \tag{6}$$

where $\tilde{\epsilon}^{-1}(\mathbf{r})$ denotes the inverse of the (position-dependent) dielectric tensor $\tilde{\epsilon}(\mathbf{r})$. In component form this may be written as

$$e_{ijk}e_{lmn}\frac{\partial}{\partial r_j}\left[\{\tilde{\epsilon}^{-1}(\mathbf{r})\}_{kl}\frac{\partial}{\partial r_m}H_n(\mathbf{r})\right]=\frac{\omega^2}{c^2}H_i\ . \tag{7}$$

Because the composite is periodic, $\mathbf{H}$ must be a Bloch function. Hence, it can be expressed as a linear combination of plane waves:

$$\mathbf{H}_{\mathbf{k}}(\mathbf{r})=\sum_{\mathbf{G}}\mathbf{H}_{\mathbf{k}+\mathbf{G}}e^{i(\mathbf{k}+\mathbf{G})\cdot\mathbf{r}}\ . \tag{8}$$

The matrix $\tilde{\epsilon}^{-1}(\mathbf{r})$ is also periodic and can be expanded as

$$\tilde{\epsilon}^{-1}(\mathbf{r})=\sum_{\mathbf{G}'}\tilde{\epsilon}^{-1}(\mathbf{G}')e^{i\mathbf{G}'\cdot\mathbf{r}}\ . \tag{9}$$

Here $\mathbf{G}$ and $\mathbf{G}'$ are reciprocal-lattice vectors, and $\mathbf{k}$ is a Bloch vector. Note that $\tilde{\epsilon}^{-1}(\mathbf{G}')$ is the Fourier transform of $\tilde{\epsilon}^{-1}(\mathbf{r})$, and is *not* equivalent to $[\tilde{\epsilon}(\mathbf{G}')]^{-1}$.

For a two-component composite, $\epsilon(\mathbf{r})$ takes the form

$$\tilde{\epsilon}(\mathbf{r})=\tilde{\epsilon}_m+\Theta(\mathbf{r})(\tilde{\epsilon}_s-\tilde{\epsilon}_m)\ , \tag{10}$$

where

$$\Theta(\mathbf{r})=\begin{cases}1 & \text{if } \mathbf{r} \text{ is inside medium } s,\\ 0 & \text{otherwise}\ ,\end{cases} \tag{11}$$

is a function introduced by Bergman.[20] If we assume a geometry in which spheres of dielectric tensor $\tilde{\epsilon}_s$ and radius R are embedded in a host of dielectric tensor $\tilde{\epsilon}_m$, then

$$\Theta(\mathbf{r})=\sum_{\mathbf{r}_L}\Theta_s(R-|\mathbf{r}-\mathbf{r}_L|)\ , \tag{12}$$

where $\mathbf{r}_L$ is the position of the Lth sphere and

$$\Theta_s(x)=\begin{cases}1, & x>0,\\ 0, & x<0\ .\end{cases} \tag{13}$$

Note that form (10) implies that the optical axes of all the spheres are aligned in the same directions.

For this geometry, the inverse of $\tilde{\epsilon}(\mathbf{r})$ takes the form

$$\tilde{\epsilon}^{-1}(\mathbf{r})=\tilde{\epsilon}_m^{-1}+\Theta(\mathbf{r})(\tilde{\epsilon}_s^{-1}-\tilde{\epsilon}_m^{-1})\ . \tag{14}$$

With the use of the property $\Theta^2=\Theta$, it is readily verified that

$$\tilde{\epsilon}(\mathbf{r})\tilde{\epsilon}^{-1}(\mathbf{r})=\tilde{1} \tag{15}$$

as required, where $\tilde{1}$ is the unit matrix.

Substituting Eqs. (8) and (9) into Eq. (7), and Fourier transforming, we find a linear system of equations (taking $c=1$):

$$\sum_{\mathbf{G}}e_{ijk}e_{lmn}(\mathbf{k}+\mathbf{Q})_j[\tilde{\epsilon}^{-1}(\mathbf{Q}-\mathbf{G})]_{kl}(\mathbf{k}+\mathbf{G})_m[\mathbf{H}_{\mathbf{k}+\mathbf{G}}]_n=\omega^2[\mathbf{H}_{\mathbf{k}+\mathbf{Q}}]_i\ . \tag{16}$$

The Fourier transform of $\tilde{\epsilon}^{-1}(\mathbf{r})$ is

$$\tilde{\epsilon}^{-1}(\mathbf{q})=\delta_{\mathbf{q},0}\tilde{\epsilon}_m^{-1}+(\tilde{\epsilon}_s^{-1}-\tilde{\epsilon}_m^{-1})f(q)\ , \tag{17}$$

where, for a diamond lattice of spheres,

$$f(q)=S(q)\frac{4\pi R^3}{v_c}\frac{j_1(qR)}{qR} . \quad (18)$$

Here v_c is the fcc primitive cell volume, and j_1 is a spherical Bessel function of order 1. $S(q)=\sum_{j=1}^{2}e^{-i\mathbf{q}\cdot\mathbf{d}_j}$ is the structure factor for the diamond lattice, the $\mathbf{d}_j$ being the positions of the basis "atoms" in the diamond structure.

Equations (16) can be expressed in the matrix form, $\sum_{j,\mathbf{G}}\tilde{M}_{ij}(\mathbf{H}_{\mathbf{k}+\mathbf{G}})_j=\omega^2(\mathbf{H}_{\mathbf{k}+\mathbf{Q}})_i$, where

$$[\tilde{M}(\mathbf{Q},\mathbf{G})]_{ij}=e_{lpj}e_{ink}(\mathbf{k}+\mathbf{Q})_n(\mathbf{k}+\mathbf{G})_p\{\delta_{\mathbf{Q},\mathbf{G}}(\tilde{\epsilon}_m^{-1})_{kl}+[(\tilde{\epsilon}_s^{-1})_{kl}-(\tilde{\epsilon}_m^{-1})_{kl}]f(|\mathbf{Q}-\mathbf{G}|)\} . \quad (19)$$

The $\omega(k)$ dispersion relation is then found by diagonalizing the matrix $\tilde{M}$. For N reciprocal-lattice vectors $\mathbf{G}$, this requires diagonalizing a $3N\times 3N$ matrix.

For materials with natural optical activity, $\tilde{\epsilon}^{-1}(\mathbf{r})$ must be construed as an operator. To first order in ηk, it can be approximated as

$$[\tilde{\epsilon}^{-1}(\mathbf{r})]_{ij}=\frac{1}{\epsilon^{(0)}}\left[\delta_{ij}-\frac{\eta}{\epsilon^{(0)}}e_{ijl}\frac{\partial}{\partial r_l}\right] . \quad (20)$$

To verify this, one can let the product $\tilde{\epsilon}\tilde{\epsilon}^{-1}$ act on a vector plane wave $\mathbf{V}e^{i\mathbf{k}\cdot\mathbf{r}}$:

$$\begin{aligned}\tilde{\epsilon}_{ij}\tilde{\epsilon}^{-1}_{jm}V_m e^{i\mathbf{k}\cdot\mathbf{r}}&=\epsilon^{(0)}\left[\delta_{ij}+\frac{ie_{ijl}\eta k_l}{\epsilon^{(0)}}\right]\\&\quad\times\frac{1}{\epsilon^{(0)}}\left[\delta_{jm}-\frac{ie_{jmp}\eta k_p}{\epsilon^{(0)}}\right]V_m e^{i\mathbf{k}\cdot\mathbf{r}}\\&\approx\delta_{im}V_m e^{i\mathbf{k}\cdot\mathbf{r}} . \quad (21)\end{aligned}$$

The inverse dielectric tensor of the composite takes the form

$$[\tilde{\epsilon}^{-1}(\mathbf{r})]_{ij}=\delta_{ij}+\Theta_s(\mathbf{r})\left[\frac{1}{\epsilon^{(0)}}\left[\delta_{ij}-\frac{\eta}{\epsilon^{(0)}}e_{ijl}\frac{\partial}{\partial r_l}\right]-\delta_{ij}\right] , \quad (22)$$

where it has been assumed that the spheres are embedded in air. The analog of Eq. (16) for naturally optically active spheres is then

$$-\sum_{\mathbf{G}}e_{pqi}e_{jmn}[\tilde{\epsilon}^{-1}(\mathbf{Q}-\mathbf{G})]_{ij}(\mathbf{k}+\mathbf{G})_q(\mathbf{k}+\mathbf{G})_m(\mathbf{H}_{\mathbf{k}+\mathbf{G}})_n=\omega^2(\mathbf{H}_{\mathbf{k}+\mathbf{Q}})_p , \quad (23)$$

where

$$[\tilde{\epsilon}^{-1}(\mathbf{Q}-\mathbf{G})]_{ij}=\delta_{ij}\delta_{\mathbf{Q},\mathbf{G}}+f(\mathbf{Q}-\mathbf{G})\delta_{ij}\left[\frac{1}{\epsilon^{(0)}}-1\right]-f(\mathbf{Q}-\mathbf{G})\frac{ie_{ijl}\eta(\mathbf{k}+\mathbf{G})_l}{\epsilon^{(0)}} . \quad (24)$$

In performing our calculations, we have generally used $N=169$ plane waves. According to Sözüer, Haus, and Inguva[16,21] many more plane waves may be needed to achieve good convergence. Ho, Chan, and Soukoulis,[5] in their original study of the close-packed diamond structure (sphere filling fraction $f=0.34$, isotropic spheres of $\epsilon_s=12.96$ in air), found a gap-to-midgap ratio $\Delta\omega/\omega_g$ of about 0.15 ($\Delta\omega$ is the frequency range with zero photonic density of states, and ω_g is the midgap frequency). They use about 375 plane waves, and in addition to calculating $\tilde{\epsilon}(\mathbf{r})$ on a discrete grid of points, they make the approximation $\tilde{\epsilon}^{-1}(\mathbf{q})\approx[\tilde{\epsilon}(\mathbf{q})]^{-1}$. According to Sözüer, Haus, and Inguva, this approximation leads to further convergence problems. For the same structure, without making this assumption, they find $\lim_{N\to\infty}\Delta\omega/\omega_g=0.035$. Calculating $\tilde{\epsilon}^{-1}(\mathbf{q})$ directly and using $N=169$, we find $\Delta\omega/\omega_g=0.0696$ for this composite.

Although our results for isotropic spheres would undoubtedly reduce to those of Ref. 21 in the limit $N\to\infty$, we use $N=169$ in the interest of using a reasonable amount of computer time while still seeing qualitative effects of anisotropic dielectric constants. For moderately anisotropic spheres, we find that the gaps converge with increasing N at a rate similar to or slightly slower than the isotropic case. For uniaxial spheres with $\epsilon_{yy}=\epsilon_{zz}=12.96$ and $\epsilon_{xx}=9$, a photonic gap persists up to $N=941$, the largest number of plane waves we have considered.

Figure 1 shows the well-known Brillouin zone of the fcc lattice (the Bravais lattice for the diamond structure), with important symmetry directions indicated. The introduction of anisotropy reduces the crystal symmetry so that many previously equivalent directions in k space become inequivalent. For instance, the bands along ΓX differ, in general, for X in the (100), (010), and (001) directions. Because of this we will present band structures along the directions of Fig. 1, but sometimes with several choices for the optical axes of the inclusions.

For N plane waves, we always find $2N$ nonzero bands, and N identically zero bands. The $2N$ bands correspond to the two transverse modes which propagate for each wave vector in a homogeneous dielectric while the N zero modes correspond to the longitudinal modes.

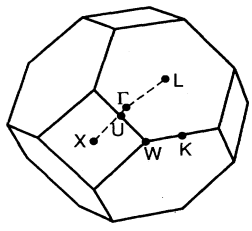

FIG. 1. fcc Brillouin zone. The labeled symmetry points are $\Gamma=(0,0,0)$, $X=(2\pi/a)(0,0,1)$, $W=(2\pi/a)(\frac{1}{2},0,1)$, $K=(2\pi/a)(\frac{3}{4},0,\frac{3}{4})$, $L=(2\pi/a)(\frac{1}{2},\frac{1}{2},\frac{1}{2})$, $U=(2\pi/a)(\frac{1}{4},\frac{1}{4},1)$, where a is the lattice constant.

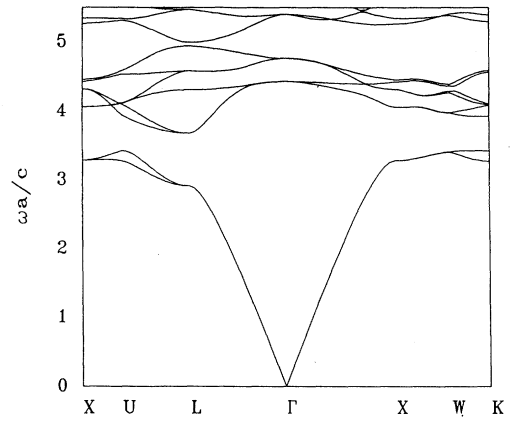

FIG. 2. Photonic band structure for a close-packed diamond lattice of isotropic dielectric spheres in air. The sphere dielectric constant is $\epsilon_s = 12.96$.

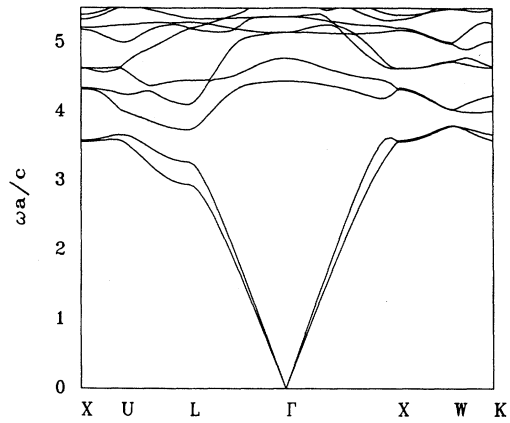

FIG. 4. Same as Fig. 3, but $\epsilon_{xx} = 6.0$, $\epsilon_{yy} = \epsilon_{zz} = 12.96$.

IV. BAND STRUCTURES FOR UNIAXIAL AND BIAXIAL SPHERES

Figure 2 shows the calculated photonic band structure of a close-packed diamond structure of isotropic spheres ($\epsilon_s = 12.96$) in air ($\epsilon_a = 1.0$). The frequencies ω are given in units of c/a, where a is the lattice constant. The lowest four nonzero bands are twofold degenerate along ΓL, ΓX, and XW. We have calculated the corresponding band structures for uniaxial spheres with $\epsilon_{yy} = \epsilon_{zz} = 12.96$ and $6.0 \leq \epsilon_{xx} \leq 12.0$. Figures 3 and 4 show the resulting band structures for $\epsilon_{xx} = 9.0$ and 6.0. The corresponding gap-to-midgap ratio $\Delta\omega/\omega_g$ is plotted in Fig. 5. With sufficient anisotropy ($\Delta\epsilon \equiv \epsilon_{zz} - \epsilon_{xx} > 7$) the full gap closes, but gaps remain along some directions in k space, producing a band structure analogous to that of a semimetal. The curve of Fig. 5 (for $\Delta\epsilon \leq 7$ and $N = 169$) can be fit to a parabola: $\Delta\omega/\omega_g = 0.691 - (5.72 \times 10^{-3})\Delta\epsilon - (8.69 \times 10^{-4})(\Delta\epsilon)^2$.

The gap is narrowed because several degenerate bands (e.g., the lowest two in Figs. 3 and 4) are split by anisotropy. This is analogous to the splitting of electronic states by an external field (Stark or Zeeman effect). The anisotropy also eliminates many level crossings. Typically, under this perturbation, two nearby levels repel each other. This is analogous to the well-known effect of perturbations in quantum calculations. Note that in our calculations, the bands along XW do not split. The reason is that along XW, $\mathbf{k}$ is parallel to $\hat{\mathbf{x}}$, the direction of the optical axis. Any wave propagating with $\mathbf{k}$ off the optical axis, however, can have two different frequencies.

At long wavelengths ($\omega \to 0$) we can determine the group velocities of the propagating modes from the slopes $d\omega/dk$ of the "valence" bands along ΓX and ΓL. Table I lists the effective "indices of refraction" $n_e \equiv \lim_{k \to 0}[c(d\omega/dk)^{-1}]$ for composites with uniaxial spheres, along ΓX and ΓL. In each direction there are two different indices of refraction, n_{e1} and n_{e2}; n_{e1} (but not n_{e2}) is independent of direction. These waves are analogous to ordinary and extraordinary rays in a homo-

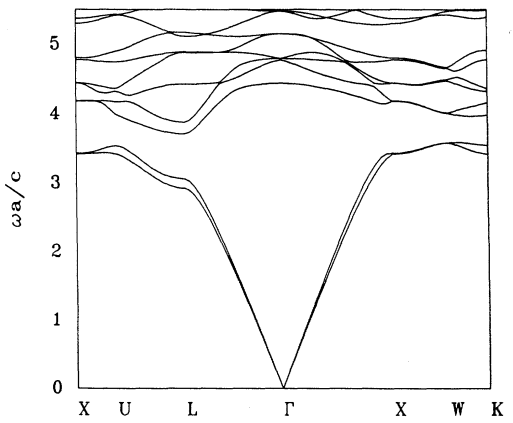

FIG. 3. As in Fig. 2 but for a close-packed diamond structure lattice of uniaxial dielectric spheres $\epsilon_{xx} = 9.0$, $\epsilon_{yy} = \epsilon_{zz} = 12.96$.

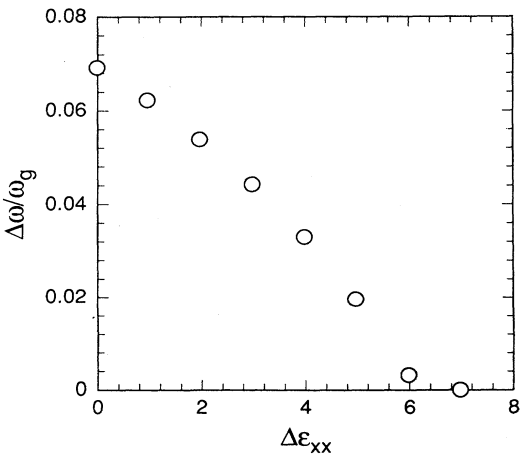

FIG. 5. Gap-to-midgap ratio $\Delta\omega/\omega_g$ vs anisotropy $\Delta\epsilon = \epsilon_{zz} - \epsilon_{xx}$, with $\epsilon_{yy} = \epsilon_{zz} = 12.96$, for uniaxial spheres in air.

TABLE I. Long-wavelength refractive indices for composites with optically uniaxial spheres. $\Delta\epsilon=\epsilon_{yy}-\epsilon_{xx}$ is a measure of the anisotropy. n_{e1} and n_{e2} correspond to the first and second nonzero bands. $[n_{e0}]_{MG}$ and $[n_0]_{MG}$ are the corresponding Maxwell-Garnett indices [Eqs. (25)–(27)]. Note that $[n_0]_{MG}$ is direction independent.

	$\Gamma X[\mathbf{k}\|(001)]$			$\Gamma L[\mathbf{k}\|(111)]$			
$\Delta\epsilon$	n_{e1}	n_{e2}	$[n_{e0}]_{MG}$	n_{e1}	n_{e2}	$[n_{e0}]_{MG}$	$[n_0]_{MG}$
0.0	1.533	1.533	1.456	1.533	1.533	1.456	1.456
0.96	1.531	1.519	1.447	1.531	1.522	1.450	1.456
1.96	1.529	1.503	1.437	1.529	1.511	1.443	1.456
2.96	1.527	1.485	1.424	1.527	1.498	1.434	1.456
3.96	1.525	1.464	1.409	1.525	1.483	1.424	1.456
4.96	1.523	1.440	1.392	1.523	1.466	1.412	1.456
5.96	1.520	1.412	1.371	1.520	1.445	1.397	1.456
6.96	1.517	1.378	1.345	1.517	1.420	1.379	1.456

geneous, uniaxial dielectric, which also have two indices of refraction, one direction independent ("ordinary") and one direction independent ("extraordinary").[17]

We can estimate n_{e1} and n_{e2} from the well-known Maxwell-Garnett approximation (MGA), suitably extended to uniaxially anisotropic spherical inclusions in an isotropic host.[22] If the spheres have principal dielectric constants $\epsilon_\perp$ and $\epsilon_\parallel$ perpendicular and parallel to the optic axis, then the principal components of the MGA are

$$[\epsilon_{\perp,\parallel}]_{MG}=\frac{\epsilon_{\perp,\parallel}(1+2f)+2(1-f)}{\epsilon_{\perp,\parallel}(1-f)+f+2}\ , \tag{25}$$

where f is the volume fraction of spheres. These would produce ordinary and extraordinary waves with indices of refraction

$$[n_0]_{MG}=\sqrt{(\epsilon_\perp)_{MG}}\ , \tag{26}$$

$$[n_{e0}]_{MG}=\left[\frac{\sin^2\theta}{(\epsilon_\parallel)_{MG}}+\frac{\cos^2\theta}{(\epsilon_\perp)_{MG}}\right]^{-1/2}\ , \tag{27}$$

where θ is the angle between the wave vector $\mathbf{k}$ and the optic axis (the x axis).

Table I lists the indices of refraction $[n_0]_{MG}$ and $[n_{e0}]_{MG}$ for waves propagating in the ΓX direction ($\theta=0$) and ΓL direction ($\theta=0.9553$ rad), as calculated from Eqs. (25)–(27). For both waves, and along both directions, the Maxwell-Garnett predictions agree with the band-structure calculations to within about 5%. The agreement might improve even further if more plane waves were included in Eqs. (8) and (9). Perfect agreement is not expected, however, since the MGA applies best to composites with isolated spheres, whereas in the present model, each sphere touches four others.

Figure 6 shows the band structure for a diamond lattice of HgS (cinnabar) spheres ($\epsilon_\perp=8.145$, $\epsilon_\parallel=10.25$)[23] in air. The three plots correspond to the optical axis of the HgS spheres parallel to the x, y, and z directions (the point X is always along the [001] direction as above). In each case, some of the degeneracies seen in the isotropic case remain unsplit in the composite. For example, in Fig. 6(b), the bands along ΓX do not split because this is the direction of the optical axis. All band structures reveal a gap throughout the Brillouin zone, but the gap width depends on the direction of $\mathbf{k}$ relative to the direction of the optical axis. The "forbidden gap" is, of course, no larger than the smallest of these ($\Delta\omega/\omega_g=0.044$). The corresponding indices of refraction for the lowest two bands are shown in Table II. Again, they agree well with the Maxwell-Garnett predictions.

The eigenvectors in Eq. (16) describe the wave polarizations. In uniaxial composites, we find $\mathbf{H}_{\mathbf{k}+\mathbf{G}}\|(\mathbf{k}+\mathbf{G})$ for the N zero-frequency bands. The other $2N$ nonzero modes satisfy $(\mathbf{k}+\mathbf{G})\cdot\mathbf{H}_{\mathbf{k}+\mathbf{G}}=0$. Hence, they are transverse in the sense that $\nabla\cdot\mathbf{H}=0$. The Fourier components are also real and orthogonal; that is, for two bands m and n $\sum_{\mathbf{G}}(\mathbf{H}_{\mathbf{k}+\mathbf{G}})_n\cdot(\mathbf{H}_{\mathbf{k}+\mathbf{G}})_m=h\delta_{nm}$, where h is real. The reality of $\mathbf{H}_{\mathbf{k}+\mathbf{G}}$ implies that the magnetic field is linearly polarized. Since each band has a different polarization vector, the band splitting by anisotropy implies different gaps for waves of different polarizations, a property which might prove useful for filtering applications.

Figure 7 shows the band structure for a diamond structure of close-packed biaxial spheres in air. For the principal components of ϵ, we use $\epsilon_1=10.20$, $\epsilon_2=18.52$, and $\epsilon_3=19.89$, corresponding to (aligned) spheres of stibnite.[23] We have calculated the photonic band structure along the directions shown in Fig. 1 for the six different permutations of the sphere axes. Figure 7 shows two of these band structures: (a) $\epsilon_{xx}=18.52$, $\epsilon_{yy}=19.89$, $\epsilon_{zz}=10.2$, and (b) $\epsilon_{xx}=10.2$, $\epsilon_{yy}=18.52$, $\epsilon_{zz}=19.89$. Both figures reveal the usual band splittings.

To determine if this band structure has a full photonic gap, we have computed the photonic density of states. We use a mesh of 877 k points uniformly distributed in the first Brillouin zone. The results are shown in Fig. 8. The density of states is low but nonzero near $\omega a/c\sim 3.3$ [where a gap seems to exist in Fig. 7(a)]. There is a full gap, however, only near $\omega a/c\sim 4.7$ (between the eighth and ninth bands). The seemingly zero density of states for very low frequencies ($\omega a/c<1$) is an artifact of having an insufficiently fine grid of k points. The density of states is obviously nonzero at such frequencies, as can be seen from the band structures of Fig. 7.

The long-wavelength indices of refraction (not shown) differ from the uniaxial case in that both n_{e1} and n_{e2} (the indices of the lowest two bands) depend on k direction.

As in the uniaxial case, we find that the magnetic fields for biaxial composites are transverse and linearly polarized.

V. BAND STRUCTURES FOR FARADAY-ACTIVE AND NATURALLY OPTICALLY ACTIVE MATERIALS

Next, we consider a diamond-structure composite ($f=0.34$), containing isotropic, Faraday-active spheres

TABLE II. Long-wavelength indices of refraction for a composite of HgS spheres in air. The three cases correspond to different orientations of the optical axis. n_{e1} and n_{e2} correspond to the lowest two nonzero bands.

			$\Gamma X[\mathbf{k}\|(001)]$		$\Gamma L[\mathbf{k}\|(111)]$	
ϵ_{xx}	ϵ_{yy}	ϵ_{zz}	n_{e1}	n_{e2}	n_{e1}	n_{e2}
10.246	8.145	8.145	1.474	1.435	1.460	1.434
8.145	10.246	8.145	1.474	1.435	1.460	1.434
8.145	8.145	10.246	1.434	1.434	1.460	1.434

in the presence of a magnetic field $\mathbf{H}=H\hat{\mathbf{z}}$. The spheres are assumed to have dielectric function

$$(\tilde{\epsilon}_s)_{xx}=(\tilde{\epsilon}_s)_{yy}=(\tilde{\epsilon}_s)_{zz}=\epsilon^{(0)}\ ,$$
$$(\tilde{\epsilon}_s)_{xy}=-(\tilde{\epsilon}_s)_{yx}=i\beta\ . \tag{28}$$

We arbitrarily choose $\epsilon^{(0)}=12.96$, and vary β. Our choice of $\epsilon^{(0)}$ is on the order of that of Ge below the band gap. The values of β are arbitrary and chosen simply to illustrate the effect of applying a stronger external field ($\beta \propto H$). As β increases the photonic gap converges more slowly with N, but the β dependence of the band struc-

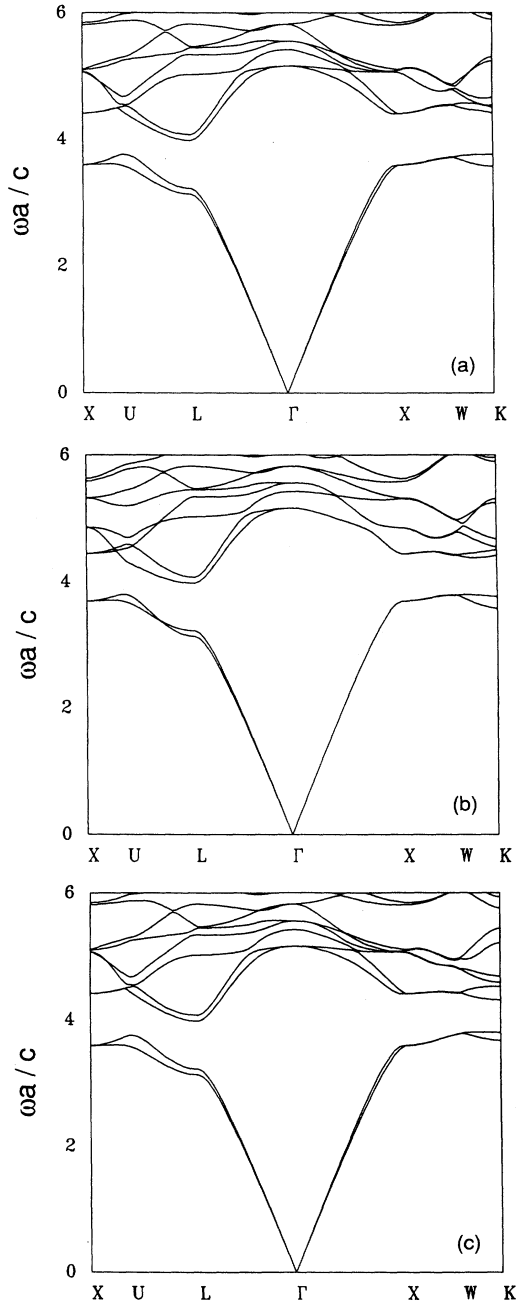

FIG. 6. As in Fig. 2 but for HgS (uniaxial) spheres in air, with (a) $\epsilon_{xx}=10.246$, $\epsilon_{yy}=\epsilon_{zz}=8.145$; (b) $\epsilon_{xx}=\epsilon_{yy}=8.145$, $\epsilon_{zz}=10.246$; and (c) $\epsilon_{xx}=\epsilon_{zz}=8.145$, $\epsilon_{yy}=10.246$.

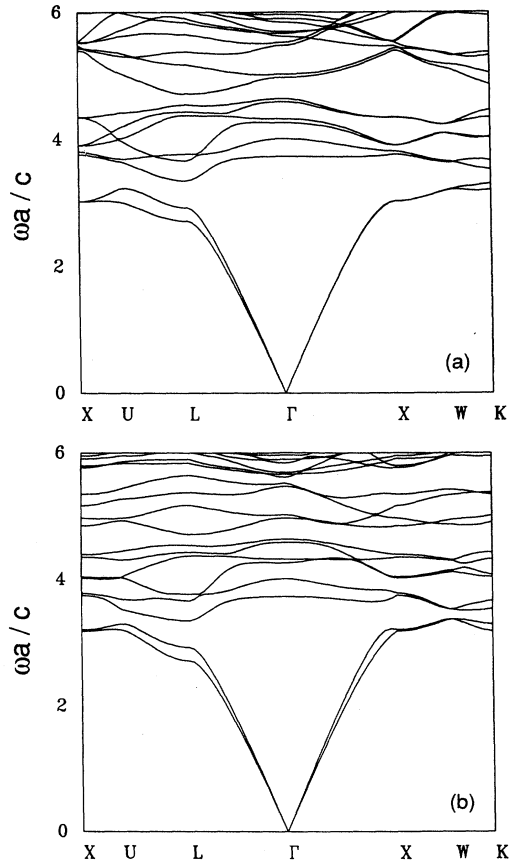

FIG. 7. As in Fig. 2 but for stibnite (biaxial) spheres in air, with (a) $\epsilon_{xx}=18.52$, $\epsilon_{yy}=19.89$, $\epsilon_{zz}=10.2$; and (b) $\epsilon_{xx}=10.2$, $\epsilon_{yy}=18.52$, $\epsilon_{zz}=19.89$.

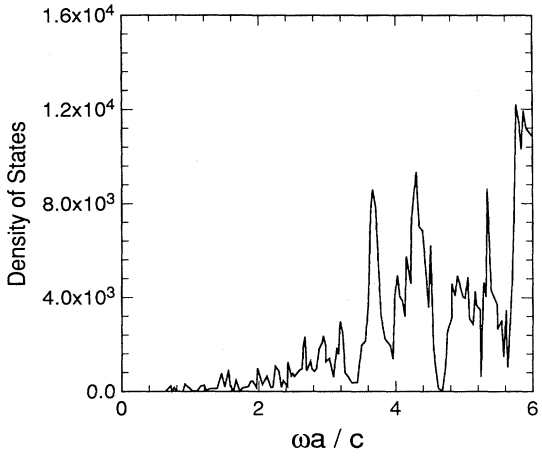

FIG. 8. Density of states per primitive cell for the composite of Fig. 7, calculated using a uniform mesh of 877 k points in the first Brillouin zone.

TABLE III. Gap-to-midgap ratio and long-wavelength indices of refraction for a composite of Faraday-active spheres in air. $\epsilon^{(0)}$ and β are defined in Eqs. (28). n_{e1} and n_{e2} correspond to the lowest two nonzero bands.

			$\Gamma X[\mathbf{k}\|(001)]$		$\Gamma L[\mathbf{k}\|(111)]$	
$\epsilon^{(0)}$	β	$\Delta\omega/\omega_g$	n_{e1}	n_{e2}	n_{e1}	n_{e2}
12.96	3.0	0.043	1.561	1.488	1.547	1.504
12.96	6.0	0.001	1.576	1.415	1.552	1.454
12.96	9.0	no gap	1.577	1.288	1.545	1.357

ture should be qualitatively correct even for $N=169$.

Figures 9(a) and 9(b) show band structures for $\beta=3.0$ and 9.0. As expected, increasing β increases the field-induced band splitting. For $\beta \geq 9.0$, the photonic gap is closed. These effects are all qualitatively similar to those seen in uniaxial and biaxial spheres. In this case, however, the composite itself is isotropic and the anisotropy is provided by an external magnetic field.

Table III lists the long-wavelength refractive indices for the lowest two bands. In contrast to the uniaxial case, *both* indices are direction dependent. This is consistent with the behavior expected in homogeneous Faraday-active media.

The band eigenvectors for Faraday-active composites are transverse in the sense that $(\mathbf{k}+\mathbf{G})\cdot\mathbf{H}_{\mathbf{k}+\mathbf{G}}=\mathbf{0}$. The individual components $\mathbf{H}_{\mathbf{k}+\mathbf{G}}$ are complex, indicating that electromagnetic waves propagating through these composites are elliptically polarized in general.

Finally, we have computed the photonic band structure for a composite with naturally optically active spheres. We use $\epsilon^{(0)}=12.96$ and $\eta=0.01$ [cf. Eq. (3)]. The band structure is shown in Fig. 10. Since $\eta|\mathbf{k}+\mathbf{G}|$ is small for most $\mathbf{G}$, the band structure closely resembles the isotropic case with $[\epsilon_s]_{ij}=(12.96)\delta_{ij}$. The long-wavelength refractive indices also prove to be the same as in the isotropic case, to within numerical accuracy, although at higher frequencies the optically active band structure shows some band splitting not evident in the

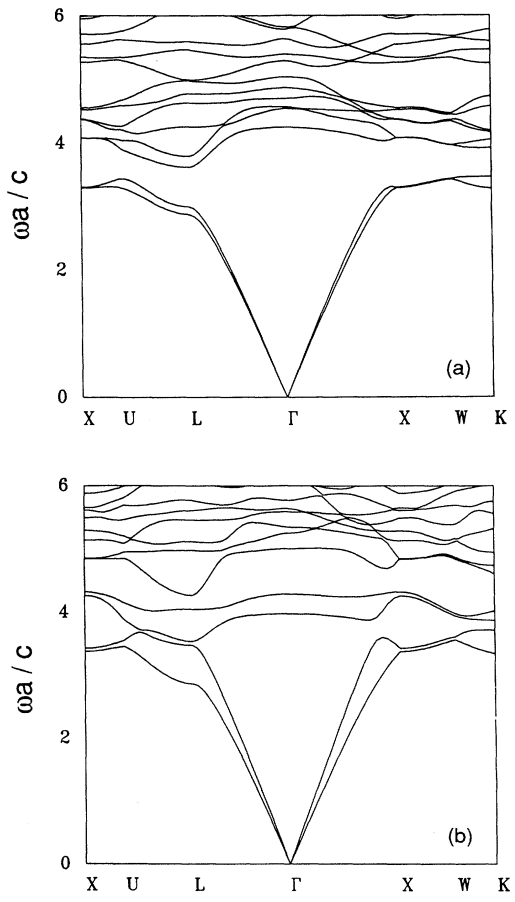

FIG. 9. As in Fig. 2, but for Faraday-active spheres in air, with $\epsilon^{(0)}=12.96$ and (a) $\beta=3.0$, (b) $\beta=9.0$.

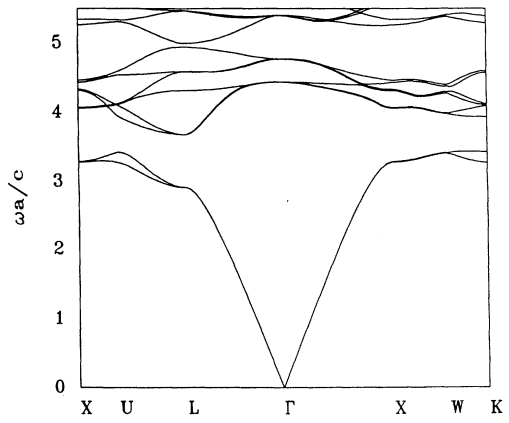

FIG. 10. As in Fig. 2 but for naturally optically active spheres in air, with $\epsilon^{(0)}=12.96$ and $\eta=0.01$.

isotropic case (cf. Figs. 2 and 10). The Fourier components $\mathbf{H}_{\mathbf{k}+\mathbf{G}}$ are complex, implying that electromagnetic waves in the composite are elliptically polarized.

VI. SUMMARY

We have shown that a plane-wave expansion method can be used to calculate the photonic band structure of an ordered composite, even if the constituents are optically anisotropic. We have applied this method to materials which are optically uniaxial, biaxial, Faraday-active, or naturally optically active. In all cases, anisotropy splits degenerate bands, and narrows any photonic band gap. With sufficient anisotropy, gaps may close up altogether.

Some of the geometries discussed may appear arbitrary and unphysical—e.g., a lattice of aligned uniaxial spheres. We expect, however, similar effects in other geometries which may be easier to achieve experimentally, such as the inverse situation, where spheres (or nonspherical regions) are carved out of a matrix of anisotropic material. In addition, anisotropy could be achieved by applying a static electric or magnetic field to a composite with *isotropic* components. If the spheres exhibit a sufficiently large Kerr, Pockels, or Faraday effect, substantial optical anisotropy could be achieved.

We can easily estimate the field strength required to observe the effects of anisotropy in a photonic crystal. Ge may be a useful material for this purpose; it has a sufficiently large index of refraction that a photonic crystal of Ge and air will have a band gap. *N*-type Ge has a room-temperature microwave Faraday effect. At a field of 0.83 T and a frequency of 24.9 GHz, for instance, it has a specific rotation of about 0.28 rad/mm.[24] If an external field is applied along the (001) direction of a Ge/air photonic crystal, and if this direction is also the Ge(001) direction, then the composite is effectively isotropic, and the specific rotation ϕ/l can be expressed as in Eq. (2):[17]

$$\frac{\phi}{l}=\frac{\omega\beta}{2cn_0}\ , \tag{29}$$

where n_0 is the index of refraction of the inclusions (≈ 4 for Ge). Substitution of these parameters into Eq. (29) gives $\beta=4.3$, a value which gives observable magnetic-field-induced band splitting according to the calculations of Sec. V. When **B** is not parallel to one of the crystal (001) directions, Ge has an anisotropic Faraday effect, and the effective splitting cannot be calculated so simply. Nevertheless, our estimate for the isotropic case indicates that the effects of anisotropy on the photonic band structure should be observable in external magnetic fields of about 1 T. Since photonic gaps tend to occur at wavelengths comparable to the scatterer size, this effect should be observable for scatterers of radius ≈ 1 cm, corresponding to the wavelength of 24.9 GHz radiation.

Achieving anisotropy through the Kerr or Pockels effect may require an extremely large electric field. For example, $BaTiO_3$, which has large Pockels coefficients at visible wavelengths ($r_{42}=1.64\times10^{-9}$ m/V, $r_2=1.08\times10^{-10}$ m/V),[25] would require fields of $\sim10^7$, 10^8 V/cm in order for the anisotropic term in the dielectric constant, $r_{ij}E_j$, to be of order unity. Thus Ge in an external magnetic field may be the most promising system for observing the effects of dielectric anisotropy.

At low frequencies we find that uniaxial composites propagate waves which are analogous to ordinary and extraordinary waves. The group velocities of these waves are well described by the Maxwell-Garnett approximation. A similar approximation describes long-wavelength propagation in biaxial composites. We also find that, for both uniaxial and biaxial composites, the Bloch waves are linearly polarized, while for Faraday-active or naturally optically active composites, the waves are polarized elliptically.

A number of possible calculations suggest themselves for future work. Obviously, it would be useful to determine more accurate band gaps for real materials, perhaps by increasing the size of the plane-wave basis. It would also be of interest to consider *randomly oriented* uniaxial spheres, in which the orientational disorder could produce damping of the Bloch waves. Experimental verification of the predicted effects would also be of great interest.

ACKNOWLEDGMENTS

This work was supported by the NSF through Grant No. DMR 90-20994. Calculations were carried out on the Cray YMP 8/864 at the Ohio Supercomputer Center with the help of a grant of time. We would like to thank Professor P. M. Hui for helpful discussions, Professor J. W. Haus for informing us of his work prior to publication, and Dr. H. Zhong and J. Raynolds for providing sets of k points and for helpful discussions.

*Present address: Byrd Polar Research Center, The Ohio State University, Columbus, OH 43210.

[1]E. Yablonovitch, Phys. Rev. Lett. **58**, 2059 (1987).
[2]E. Yablonovitch and T. J. Gmitter, Phys. Rev. Lett. **63**, 1950 (1989).
[3]S. John and J. Wang, Phys. Rev. Lett. **64**, 2418 (1990).
[4]K. M. Leung and Y. F. Liu, Phys. Rev. Lett. **65**, 2646 (1990).
[5]K. M. Ho, C. T. Chan, and C. M. Soukoulis, Phys. Rev. Lett. **65**, 3152 (1990).
[6]E. Yablonovitch, T. J. Gmitter, and K. M. Leung, Phys. Rev. Lett. **67**, 2295 (1991).
[7]R. D. Meade, K. D. Brommer, A. M. Rappe, and J. D. Joannopoulos, Phys. Rev. B **44**, 10 961 (1991).
[8]R. D. Meade, K. D. Brommer, A. M. Rappe, and J. D. Joannopoulos, Phys. Rev. B **44**, 13 772 (1991).
[9]E. Yablonovitch, T. J. Gmitter, R. D. Meade, A. M. Rappe, K. D. Brommer, and J. D. Joannopoulos, Phys. Rev. Lett. **67**, 3380 (1991).
[10]S. Satpathy, Z. Zhang, and M. R. Salehpour, Phys. Rev. Lett. **64**, 1239 (1990).

[11]S. John, Phys. Today **44** (5), 32 (1991).
[12]L. Brillouin, *Wave Propagation in Periodic Structures* (McGraw-Hill, New York, 1946); W. E. Kock, Bell Syst. Tech. J **27**, 58 (1948).
[13]W. Lamb, D. M. Wood, and N. W. Ashcroft, Phys. Rev. B **21**, 2248 (1980); W. T. Doyle, in *Electrical Transport and Optical Properties of Inhomogeneous Media,* edited by J. C. Garland and D. B. Tanner (AIP, New York, 1978), p. 300; D. J. Bergman and K. J. Dunn, Phys. Rev. B **45**, 13 262 (1992).
[14]P. L. Gourney, M. E. Warren, J. R. Wendt, G. A. Vawter, T. M. Brennan, and B. E. Hammons, Am. Phys. Soc. Bull. **37**, 599 (1992).
[15]J. W. Haus, H. S. Sözüer, and R. Inguva (unpublished).
[16]H. S. Sözüer, J. W. Haus, and R. Inguva (unpublished).
[17]L. D. Landau and E. M. Lifshitz, *Electrodynamics of Continuous Media,* 2nd ed. (Pergamon, Oxford, 1984), Chaps. XI and XII.
[18]*Handbook of Chemistry and Physics* (The Chemical Rubber Company, Cleveland, 1964), p. E-226.
[19]The phrase "photonic band structure" might seem to suggest a quantum-mechanical treatment of the electromagnetic field. However, the band structures are calculated treating this field classically.
[20]D. J. Bergman, Phys. Rev. B **14**, 4304 (1976).
[21]H. S. Sözüer, J. W. Haus, and R. Inguva, Phys. Rev. B **45**, 13 962 (1992).
[22]J. C. Maxwell-Garnett, Philos. Trans. R. Soc. London **203**, 385 (1904); **205**, 237 (1906); D. Stroud and F. P. Pan, Phys. Rev. B **13**, 1434 (1976).
[23]*American Institute of Physics Handbook* (McGraw-Hill, New York, 1957), pp. 6-12 to 6-17 and 5-235.
[24]A. Bouwknegt and J. Volger, Physica **30**, 113 (1964).
[25]See *American Institute of Physics Handbook* (Ref. 23), p. 6-239.